SUPPORTING INFORMATION

Enhanced detection of quantum dots by the magnetohydrodynamic effect for electrochemical biosensing

Daniel Martín-Yerga[1], Pablo Fanjul-Bolado[2], David Hernández-Santos[2], and Agustín Costa-García[1*]*

[1] Departamento de Química Física y Analítica**,** Universidad de Oviedo, 33006 Oviedo, Asturias, Spain.

[2] DropSens, S.L., Edificio CEEI, Parque Tecnológico de Asturias, 33428 Llanera, Asturias, Spain

*E-mails: martindaniel@uniovi.es; costa@uniovi.es

REAGENTS AND SOLUTIONS

Cadmium(II) standard, mercury(II) acetate, iron(III) nitrate, d-biotin, Tris(hydroxymethyl)aminomethane (Tris), bovine serum albumin fraction V (BSA) and human serum (from human male AB plasma) were purchased from Sigma-Aldrich. Fuming hydrochloric acid (37%) was purchased from Merck. Human tissue transglutaminase (recombinantly produced in insect cells) was purchased from Zedira. Qdot® 655 streptavidin conjugate (QD-STV), biotinylated goat anti-human IgA (anti-H-IgA-BT), Qdot® 655 biotin conjugate (BT-QDs) were purchased from Life Technologies. Neutravidin was purchased from ThermoFisher Scientific. Varelisa Celikey tissue transglutaminase IgA ELISA kit was purchased from Phadia. Each kit contained six human serum calibrators (0, 3, 7, 16, 40, 100 U mL^{-1}) and a positive and a negative control. Ultrapure water obtained with a Millipore Direct Q5™ purification system from Millipore Ibérica S.A. was used throughout this work. All other reagents were of analytical grade. Working solutions of neutravidin, tTG, QD-STV, BT-QD, anti-H-IgA-BT and BSA were prepared in 0.1 M pH 7.4 Tris-HCl buffer (hereafter called Tris buffer).

IMMUNOASSAY PROCEDURES

Biotin detection was carried out following a procedure previously described by our group[1]. Briefly, an aliquot of 10 µL of $1x10^{-7}$ M neutravidin solution (in Tris) was dropped covering completely the working electrode surface. The solution was left overnight at 4 ºC in order to adsorb the protein on the electrode surface. After washing the electrode with Tris buffer, a blocking step was conducted by dropping 40 µL of a BSA solution (2.0% BSA in Tris buffer) and left to adsorb for 30 minutes. After another washing step with Tris, 30 µL of BT and BT-QDs solution (in Tris) was placed on the electrode in order to perform the affinity reaction between neutravidin and BT or BT-QDs. Free BT was only used in the competitive assay. A last washing step was carried out with ultrapure water and the electrode was left to dry and connected to the potentiostat for the voltammetric measurement using differential-

pulse anodic stripping voltammetry (DPASV). **Figure S1** shows a schematic drawing of the competitive biosensor.

Detection of anti-tTG IgA antibodies was carried out following a procedure previously described by our group[2]. Briefly, an aliquot of 10 µL of 0.1 mg/mL tTG solution (in Tris) was dropped covering completely the surface of the working electrode. The solution was left overnight at 4 ºC in order to adsorb the protein on the electrode surface. The devices were washed with Tris buffer and 40 µL of a BSA solution (2.0% BSA in Tris buffer) was dropped on the electrode and left to adsorb for 30 minutes in order to avoid non-specific adsorptions, and forming the immunosensor phase. The detection of anti-tTG IgA antibodies was carried out by incubating the immunosensor with 30 µL of serum solutions (1:2 in Tris buffer) for 60 min followed by a washing step with Tris buffer. Then, 40 µL of a 7.5 µg/mL anti-IgA-BT (with 1 mg/mL of BSA) solution were added to the sensor for 60 minutes followed by another washing step with Tris buffer. Finally, 25 µL of QDs-STV (1.5 nM in terms of QDs) were added and left to incubate for 30 minutes. A last washing step was performed with ultrapure water and the electrode was left to dry and connected to the potentiostat for the voltammetric measurement using DPASV. **Figure S2** shows a schematic drawing of the immunosensor following this methodology.

FIGURES

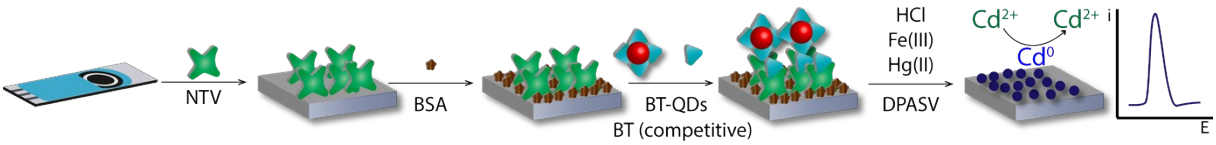

Figure S1. Scheme of the competitive biosensor between neutravidin as recognition element and biotin and biotin labelled with QDs conducted on the surface of screen-printed electrodes. Detection is carried out by ASV in a HCl solution containing Fe(III) and Hg(II).

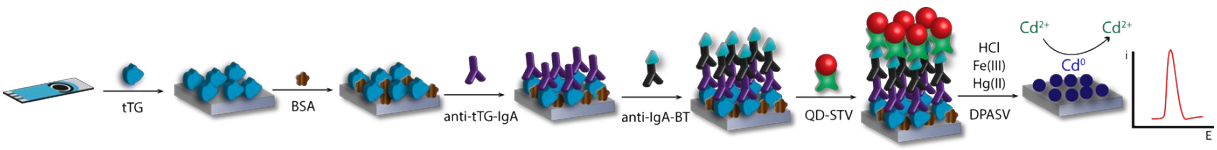

Figure S2. Scheme of the biosensor employed for the detection of anti-transglutaminase IgA antibodies. Tissue-transglutaminase is used as recognition element and the biosensor is carried out on the surface of screen-printed electrodes by incubating in different steps: serum sample, anti-IgA-BT and QDs-STV. Detection is carried out by ASV in a HCl solution containing Fe(III) and Hg(II).

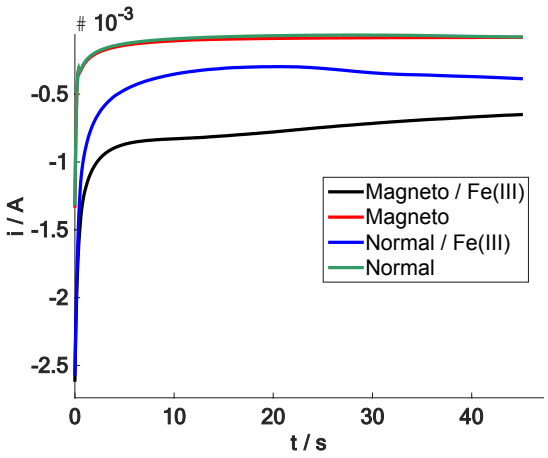

Figure S3. Chronoamperometric responses obtained for the reduction of a solution containing 100 µg/L of Cd(II), 5 mM Hg(II), 0.05 M HCl (optimized conditions) in presence and absence of 50 mM Fe(III) and in absence and presence of a magnetic field. The chronoamperometric current at 20 s was -70 µA in absence of Fe(III) and the magnetic field, -89 µA in absence of Fe(III) and presence of the magnetic field, -298 µA in presence of Fe(III) and absence of the magnetic field and -780 µA in presence of Fe(III) and the magnetic field. The cathodic current is increased in presence of Fe(III) and the magnetic field, and therefore, the Lorentz force will be able to generate a significant convective effect to enhance the mass transfer of cadmium to the electrode surface.

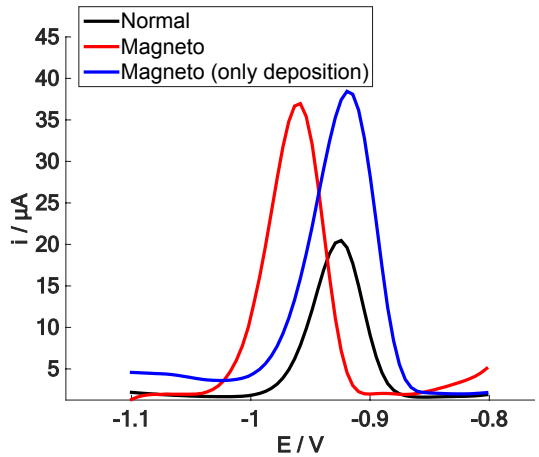

Figure S4. Differential-pulse voltammograms of a solution containing 100 µg/L Cd(II), 0.5 mM Hg(II), 50 mM Fe(III) and 0.05 M HCl (optimized conditions) in absence of the magnetic field (black line), in presence of the magnetic field only in the deposition step (blue line) and in presence of the magnetic field in the deposition and stripping steps (red line). Anodic stripping voltammetry was used in optimized conditions by applying a deposition potential of -1.1 V for 45 s.

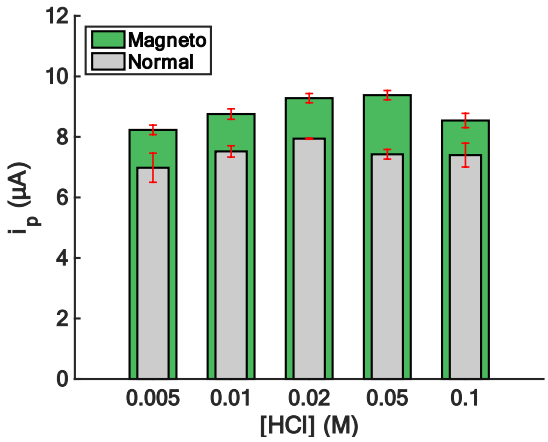

Figure S5. Effect of the HCl concentration on the stripping peak current of 100 µg/L of Cd(II) in presence and absence of a magnetic field. [Hg(II)]: 0.5 mM, [Fe(III)]: 10 mM. Deposition potential and time: -1.1 V for 45 s.

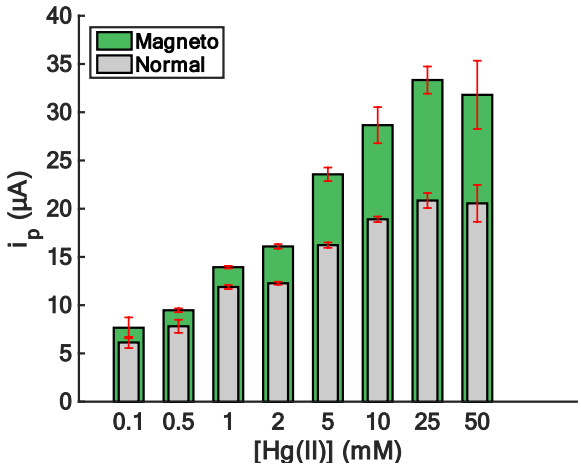

Figure S6. Effect of the Hg(II) concentration on the stripping peak current of 100 µg/L of Cd(II) in presence and absence of a magnetic field. [HCl]: 0.05 M, [Fe(III)]: 10 mM. Deposition potential and

time: -1.1 V for 45 s. Although, the peak currents increased up to 25 mM, 5 mM of Hg(II) was chosen due to the potential toxicity of this species.

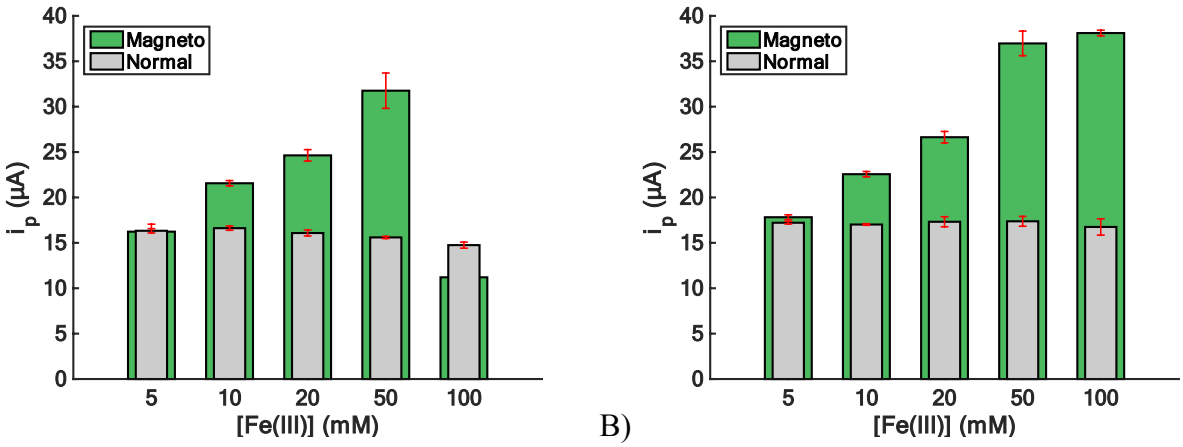

Figure S7. Effect of the Fe(III) concentration on the stripping peak current of 100 µg/L of Cd(II) in presence and absence of a magnetic field. [HCl]: 0.05 M, [Hg(II)]: 5 mM. Deposition potential and time: -1.1 V for 45 s **(A)** and -1.2 V for 45 s **(B)**.

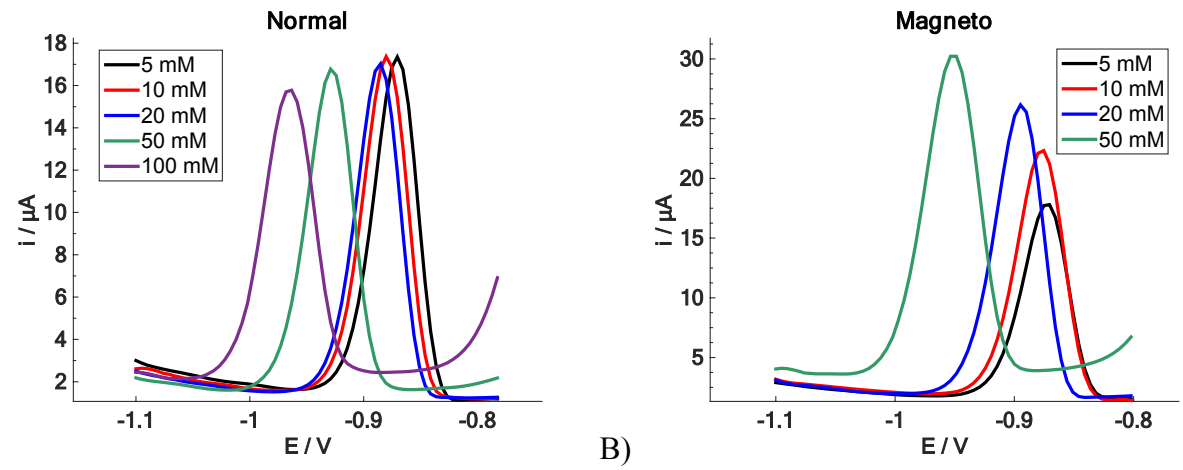

Figure S8. A) Differential-pulse voltammograms of a solution containing 100 µg/L of Cd(II), 5 mM Hg(II) and 0.05 M HCl and different concentrations of Fe(III) (5, 10, 20, 50, 100 mM) in absence of the magnetic field and **B)** in presence of the magnetic field.

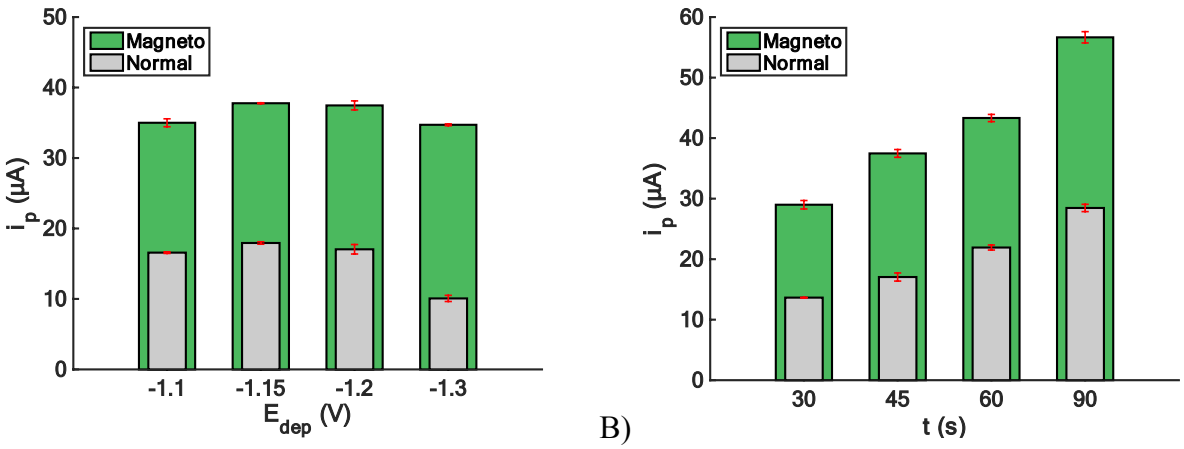

Figure S9. Effect of the deposition potential (E_{dep}) (A) and deposition time (B) on the stripping peak current of a solution containing 100 µg/L Cd(II), 5 mM Hg(II), 50 mM Fe(III) and 0.05 M HCl in presence and absence of a magnetic field. Deposition time in A) was 45 s. Deposition potential in B) was -1.1 V. Although 90 s was chosen as deposition time for the rest of the experiments, higher deposition times could be used in order to achieve a more sensitive detection.

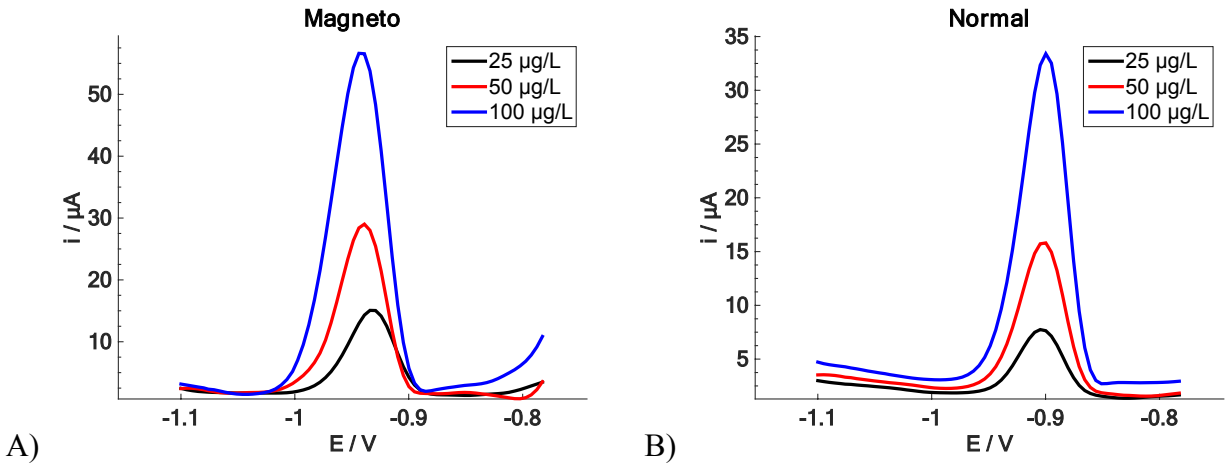

Figure S10. Differential-pulse voltammograms of solutions containing 25 µg/L (black line), 50 µg/L (red line) and 100 µg/L (blue line) of Cd(II), 5 mM Hg(II), 50 mM Fe(III), 0.05 M HCl in absence **(A)** and presence **(B)** of a magnetic field. A deposition potential of -1.1 V was applied for 90 s.

[Cd(II)]		Γ_{ads} (nmol/cm^2)	Deposition efficacy (%)
25 µg/L	Normal	0.13 ± 0.02	15.8
	Magneto	0.26 ± 0.01	17.0
50 µg/L	Normal	0.27 ± 0.02	18.3
	Magneto	0.60 ± 0.02	32.7
100 µg/L	Normal	0.56 ± 0.04	37.8
	Magneto	1.19 ± 0.05	37.3

Table S1. Values found experimentally for the surface coverage (Γ_{ads}) at different Cd(II) concentrations by using anodic stripping voltammetry (deposition: -1.1V, 90s) in presence and absence of the magnetic field. Deposition efficacy is estimated by the ratio between the deposited amount of cadmium and the initial Cd(II) present in solution.

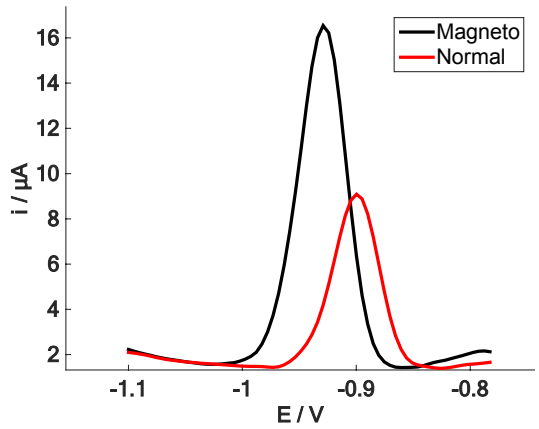

Figure S11. Differential-pulse voltammograms of a solution containing 2 µL of 1 nM QDs (in H_2O) and 45 µL of a solution containing 5 mM Hg(II), 50 mM Fe(III) and 0.05 M HCl in presence (black line) and absence (red line) of a magnetic field.

Reference	Linear range	Sensitivity	LOD
Direct detection[3]	8 - 230 µM	0.05 µA/µM	8 µM
SPCE[4]	~0.1 - 1.25 nM	7 µA/nM	< 0.1 nM
Microfluidic chip (flow)[4]	~0.1 - 1.25 nM	20 µA/nM	< 0.1 nM
Microfluidic device[5]	~0.5 - 7.5 nM	1.4 µA/nM	< 0.5 nM
QDs-HCl[6]	5 - 200 nM	0.23 µA/nM	2.6 nM
Ag@QDs[7]	0.5 - 25 nM	1.57 µA/nM	0.13 nM
This work	0.05 - 5 nM	15.5 µA/nM	0.05 nM

Table S2. Analytical characteristics of several electrochemical methods for the detection of Cd-based quantum dots reported in the literature.

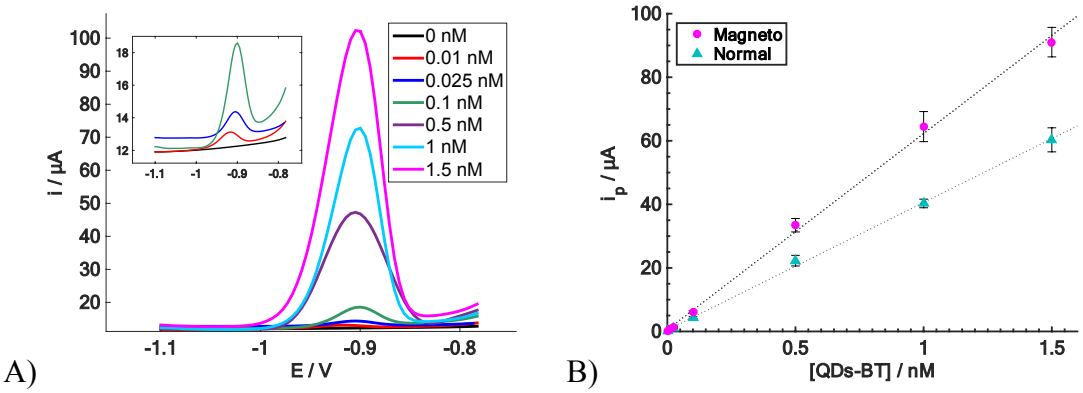

Figure S12. A) Differential-pulse voltammograms for the developed affinity biosensor for the detection of QDs-BT at different concentrations (0, 0.01, 0.025, 0.1, 0.5, 1 and 1.5 nM) in presence of the magnetic field. Inset shows the DPV responses for the lower concentrations of QDs. Procedure of the biosensor is described in section 2.3 of the main manuscript. **B)** Associated calibration plots in presence and absence of the magnetic field.

Reference	LOD (nM)	Linear range (nM)
Avidine-HRP[8]	-	285 - 8000
anti-BT and BT-liposome[9]	14	1 - 1000
MB-STV + HRP-BT[10]	84	94 - 240
MB-STV + HRP-BT (FIA)[11]	0.008	0.01 - 1
MB-STV + HRP-BT (8xSPCEs)[12]	0.2	0.2 - 250
QDs-BT-STV (8xSPCEs)[1]	1.4	1 - 100
This work	0.06	0.16 - 84.5

Table S3. Analytical characteristics of different electrochemical methods for the detection of biotin reported in the literature.

	Expected	Found	Recovery (%)
BT in multivitamin tablet	25 µg	28 ± 2 µg	102 - 115
anti-tTG IgA serum 1	5 U/mL	5.6 ± 0.3 U/mL	108 - 116
anti-tTG IgA serum 2	15 U/mL	14.8 ± 0.5 U/mL	96 - 101
anti-tTG IgA serum 3	30 U/mL	34 ± 3 U/mL	108 - 121
anti-tTG IgA positive control	26 ± 7 U/mL	27 ± 1 U/mL	-
anti-tTG IgA negative control	< 3 U/mL	1.7 ± 0.4 U/mL	-

Table S4. Values of concentration (or amount) expected for the real samples evaluated and the concentration determined experimentally by using the biosensors developed in presence of the magnetic field.

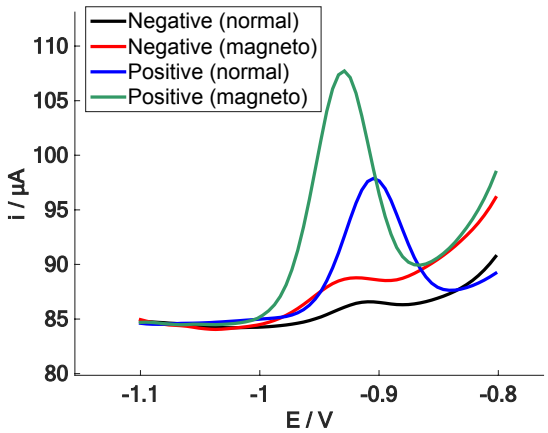

Figure S13. Differential-pulse voltammetry for the detection of anti-tTG IgA antibodies using the positive and negative serum controls in presence and absence of the magnetic field.

References

(1) Martín-Yerga, D.; González-García, M. B.; Costa-García, A. *Sens. Actuators B* **2013**, *182*, 184–189.

(2) Martín-Yerga, D.; Costa-García, A. *Bioelectrochemistry* **2015**, *105*, 88–94.

(3) Merkoçi, A.; Marcolino-Junior, L. H.; Marín, S.; Fatibello-Filho, O.; Alegret, S. *Nanotechnology* **2007**, *18* (3), 35502.

(4) Medina-Sánchez, M.; Miserere, S.; Cadevall, M.; Merkoçi, A. *Electrophoresis* **2016**, *37* (3), 432–437.

(5) Medina-Sánchez, M.; Miserere, S.; Morales-Narváez, E.; Merkoçi, A. *Biosens. Bioelectron.* **2014**, *54*, 279–284.

(6) Martín-Yerga, D.; Bouzas-Ramos, D.; Menéndez-Miranda, M.; Bustos, A. R. M.; Encinar, J. R.; Costa-Fernández, J. M.; Sanz-Medel, A.; Costa-García, A. *Electrochim. Acta* **2015**, *166*, 100–106.

(7) Martín-Yerga, D.; Rama, E. C.; Costa-García, A. *Anal. Chem.* **2016**, *88* (7), 3739–3746.

(8) Wright, J. D.; Rawson, K. M.; Ho, W. O.; Athey, D.; McNeil, C. J. *Biosens. Bioelectron.* **1995**, *10* (5), 495–500.

(9) Ho, J. A.; Hsu, W.-L.; Liao, W.-C.; Chiu, J.-K.; Chen, M.-L.; Chang, H.-C.; Li, C.-C. *Biosens. Bioelectron.* **2010**, *26* (3), 1021–1027.

(10) Kergaravat, S. V.; Gómez, G. A.; Fabiano, S. N.; Laube Chávez, T. I.; Pividori, M. I.; Hernández, S. R. *Talanta* **2012**, *97*, 484–490.

(11) Biscay, J.; González García, M. B.; Costa García, A. *Talanta* **2015**, *131*, 706–711.

(12) Biscay, J.; García, M. B. G.; García, A. C. *Sens. Actuators B* **2014**, *205*, 426–432.